

# Schaftoside improves cerebral ischemia-reperfusion injury by enhancing autophagy and reducing apoptosis and inflammation through the AMPK/mTOR pathway

Lin Zhang<sup>1,2,3,A–D</sup>, Minghua Wu<sup>1,3,A,D–F</sup>, Zhaoyao Chen<sup>1,3,A–C,F</sup>

<sup>1</sup> Department of Neurology, Affiliated Hospital of Nanjing University of Chinese Medicine, China

<sup>2</sup> Department of Neurology, Nanjing Integrated Traditional Chinese and Western Medicine Hospital Affiliated with Nanjing University of Chinese Medicine, China

<sup>3</sup> Department of Neurology, Jiangsu Province Hospital of Chinese Medicine, Nanjing, China

A – research concept and design; B – collection and/or assembly of data; C – data analysis and interpretation;

D – writing the article; E – critical revision of the article; F – final approval of the article

Advances in Clinical and Experimental Medicine, ISSN 1899–5276 (print), ISSN 2451–2680 (online)

*Adv Clin Exp Med.* 2022;31(12):1343–1354

## Address for correspondence

Minghua Wu

E-mail: minghuaw001@163.com

## Funding sources

This study was funded by the project of the Natural Science Foundation of Jiangsu Province (BK20201095), National Administration of Traditional Chinese Medicine: Evidence-Based Capacity Building Project (2019XZZX-NB007), 333 high level talents training project in Jiangsu (Grant No. BRA 2016507) and Jiangsu Province Administration of Chinese Medicine (ZT202102).

## Conflict of interest

None declared

Received on March 25, 2022

Reviewed on June 28, 2022

Accepted on July 19, 2022

Published online on September 22, 2022

## Cite as

Zhang L, Wu M, Chen Z. Schaftoside improves cerebral ischemia-reperfusion injury by enhancing autophagy and reducing apoptosis and inflammation through the AMPK/mTOR pathway. *Adv Clin Exp Med.* 2022;31(12):1343–1354. doi:10.17219/acem/152207

## DOI

10.17219/acem/152207

## Copyright

Copyright by Author(s)

This is an article distributed under the terms of the Creative Commons Attribution 3.0 Unported (CC BY 3.0) (<https://creativecommons.org/licenses/by/3.0/>)

## Abstract

**Background.** As a flavonoid compound, schaftoside (SS) possesses a wide range of pharmaceutical activities. Nonetheless, it is unclear whether SS has a neuroprotective effect in cerebral ischemia-reperfusion injury (CI/RI).

**Objectives.** To examine the neuroprotective effect of SS in CI/RI and explore the underlying mechanism.

**Materials and methods.** An in vivo middle cerebral artery occlusion (MCAO) was used to simulate CI/RI in rats. Oxygen glucose deprivation/reperfusion (OGD/R) of HT22 cells was used to establish a cellular model of CI/RI in vitro. Pathological changes were evaluated with hematoxylin and eosin (H&E) staining, apoptosis was measured using terminal deoxynucleotidyl transferase dUTP nick end labeling (TUNEL) staining and flow cytometry, and inflammatory factors were assessed using enzyme-linked immunosorbent assay (ELISA). Protein expression was detected using western blot or immunofluorescence.

**Results.** Our results indicated that SS attenuated CI/RI by improving neurologic deficits and reducing brain edema. Moreover, SS treatment blocked apoptosis and inflammation and enhanced autophagy in MCAO rats. Schaftoside was found to amplify the activation of adenosine monophosphate-activated protein kinase (AMPK)/mammalian target of rapamycin (mTOR) pathway induced by MCAO. Similarly, SS pretreatment increased cell viability and autophagy, and reduced apoptosis and inflammation in OGD/R-induced HT22 cells. The OGD/R enlarges the p-AMPK/AMPK ratio while restricting the p-mTOR/mTOR ratio, and it was found that SS further enhanced the effect of OGD/R on the AMPK/mTOR pathway. Rapamycin promoted the effect of SS on OGD/R-induced HT22 cells, while compound C produced the opposite results. Mechanistically, SS promoted autophagy and reduced apoptosis and inflammation through the regulation of the AMPK/mTOR signaling pathway.

**Conclusions.** The obtained results showed that SS protected against CI/RI through an autophagy-mediated AMPK/mTOR pathway when accessed in vitro and in vivo.

**Key words:** apoptosis, autophagy, inflammation, cerebral ischemia-reperfusion injury, schaftoside

## Background

Stroke is a central nervous system disease resulting from an acute cerebral blood circulation disorder caused by stenosis, occlusion or rupture of internal cerebral arteries.<sup>1,2</sup> Based on the pathogeny, strokes are divided into ischemic or hemorrhagic, in which ischemic strokes account for about 80% of total strokes.<sup>3</sup> The 2019 Global Stroke Statistics reported that the incidence of strokes was ranked first in China.<sup>4</sup> So far, there are no desirable drugs or strategies for the treatment of ischemic stroke. Current stroke treatment strategies include drug thrombolysis, mechanical thrombolysis, intravascular surgery, and the use of neuroprotective agents.<sup>5,6</sup> So far, recombinant tissue plasminogen activators (rtPAs), such as alteplase and reteplase, are the only drugs approved by the Food and Drug Administration (FDA) for the treatment of ischemic stroke.<sup>7</sup> However, due to the narrow treatment time window (3–4.5 h) of rtPAs and their serious adverse reactions, especially on the brain tissue injury caused by recanalization after thrombolysis by inducing a cerebral ischemia-reperfusion injury (CI/RI), the clinical application of rtPAs is limited.<sup>8</sup> The CI/RI is considered to be cell damage caused by cerebral ischemia. When blood supply is restored, the oxygen supply is enhanced and the damage to brain cells is exacerbated, resulting in further deterioration caused by the disease.<sup>9</sup> In addition, the study revealed that the ventromedial prefrontal cortex (vmPFC) is involved in the acquisition of emotional conditioning (i.e., learning), and assessed how naturally occurring bilateral lesion centered in the vmPFC compromises the generation of a conditioned psychophysiological response during the acquisition of threat conditioning (i.e., emotional learning).<sup>10,11</sup> A recent study focused on the cognitive symptoms (i.e., dysfunction in attention and emotion perception) in neurologic and brain-damaged patients, and highlighted the role of specific dysfunctional brain regions, such as the amygdala and superior temporal sulcus (STS), in the recognition and identification of nonverbal communicative signals of emotion.<sup>12</sup> The pathogenesis of neuronal damage and impairment of brain areas after stroke involves an interaction of multiple factors and pathways. Therefore, studying the pathogenesis of CI/RI is conducive to developing safe and effective drugs aimed at treating ischemic stroke.

It has been confirmed that CI/RI induces nerve cell inflammation and apoptosis or autophagy that results in neurological dysfunction.<sup>13–16</sup> Autophagy is an important stress response pathway of lysosomal degradation.<sup>17</sup> Some studies have shown that autophagy possesses a neuroprotective effect in CI/RI.<sup>18,19</sup> Melatonin can improve CI/RI in diabetic mice, and the underlying mechanism involves autophagy enhancement mediated by SIRT1/BMAL1 signaling.<sup>20</sup> Apoptosis is a kind of programmed cell death. Moreover, autophagy could block the induction of apoptosis and reduce cell damage.<sup>21</sup> Astragaloside IV has been

shown to protect against CI/RI through reducing apoptosis by promoting autophagy.<sup>22</sup> It has been reported that inflammation is enhanced in neurodegenerative diseases.<sup>23</sup> Studies have shown that inhibiting neuroinflammation is considered an important strategy for the prevention of CI/RI.<sup>24,25</sup> Hence, nerve cell apoptosis, inflammation and autophagy were analyzed in CI/RI in this paper.

Traditional Chinese medicine possesses numerous medicinal animal and plant resources.<sup>26</sup> Screening anti-CI/RI drugs derived from traditional Chinese medicine have the advantages of low toxicity and few side effects.<sup>27,28</sup> Schaftoside (SS) is a flavonoid found in a variety of Chinese herbal medicines, such as *Eleusine indica*.<sup>29</sup> Currently, SS has a wide range of pharmacological activities, including anti-inflammatory, antiviral and antioxidant properties, and the regulation of autophagy.<sup>30</sup> Polyphenols such as resveratrol can potentially lead to autophagy in many diseases.<sup>31,32</sup> It has been reported that the treatment with SS in  $\alpha$ -melanocyte-stimulating hormone ( $\alpha$ -MSH)-treated cells reduced the expression of tyrosinase and tyrosinase-related protein 1 (TRP1), and activated autophagy.<sup>30</sup> However, the effects of SS on CI/RI are still unclear.

In this paper, middle cerebral artery occlusion (MCAO) was used to simulate CI/RI in rats in vivo. Oxygen glucose deprivation/reperfusion (OGD/R) of HT22 cells was used to establish a cellular model of CI/RI in vitro. Subsequently, whether SS could alleviate a CI/RI was explored in vivo and in vitro. Moreover, the effects of SS on neuronal apoptosis, inflammation and autophagy were explored. Our results showed that SS activates the adenosine monophosphate-activated protein kinase (AMPK)/mammalian target of rapamycin (mTOR) pathway, thereby reducing apoptosis and inflammation and inducing autophagy, thus improving a CI/RI.

## Objectives

We aimed to explore whether SS could alleviate CI/RI by reducing apoptosis and inflammation and inducing autophagy through the activation of the AMPK/mTOR pathway.

## Materials and methods

### Animal experiments

Male Sprague Dawley rats (200 g,  $n = 50$ ) were obtained from the Shanghai Experimental Animal Co., Ltd. (Shanghai, China). All rats were placed in the same animal feeding facility (room temperature 18–26°C, relative humidity 40–70%, ventilation 8–12 times per hour, and light/dark cycles alternating every 12 h). As shown in Table 1, the rats were randomly divided into 5 groups ( $n = 10$  in each group): 1) sham operation group (sham

**Table 1.** The full scheme of animal experiment

Group	Time [h]		
	1	2	25
Sham (n = 10)	ig. physiological saline	Sham	ip. 120 mg/kg pentobarbital sodium
Control (n = 10)	ig. physiological saline	MCAO	ip. 120 mg/kg pentobarbital sodium
SS-L (n = 10)	ig. 50 mg/kg SS	MCAO	ip. 120 mg/kg pentobarbital sodium
SS-M (n = 10)	ig. 100 mg/kg SS	MCAO	ip. 120 mg/kg pentobarbital sodium
SS-H (n = 10)	ig. 150 mg/kg SS	MCAO	ip. 120 mg/kg pentobarbital sodium

SS – shaftoside; SS-L – SS low-dose group; SS-M – SS medium-dose group; SS-H – SS high-dose group; MCAO – middle cerebral artery occlusion; ig. – intragastrically; ip. – intraperitoneally.

group) – rats were treated by gavage with the same volume of physiological saline 1 h before modeling; 2) MCAO group – 1 h before modeling the same volume of physiological saline was given by gavage; 3) SS low-dose group (SS-L group) – 1 h before modeling the rats were treated with 50 mg/kg SS by gavage; 4) SS medium-dose group (SS-M group) – 1 h before modeling the rats were treated with 100 mg/kg of SS by gavage; 5) SS high-dose group (SS-H group) – 1 h before modeling the rats were treated with 150 mg/kg of SS by gavage.<sup>33</sup> Except for the sham group, MCAO was performed. The rats were anesthetized by intraperitoneal (ip.) injections of 10% chloral hydrate (35 mg/kg), and then the left common carotid artery (CCA), external carotid artery (ECA) and internal carotid artery (ICA) were separated. Wires were hung at the distal end and proximal end of the CCA and ECA for standby. The ICA was temporarily clamped with an arterial clamp, and the proximal CCA and ECA were ligated. Then, we cut a small opening in the ECA 4 mm away from the bifurcation of the CCA. A nylon suture was inserted from the ECA to ICA and gently fastened to a wire that was wound around the distal end of the CCA. The nylon suture was gently pushed with tweezers until an insertion depth of 18 mm was reached and slight resistance was met. The nylon suture was firmly fastened to the wire at the distal end of the CCA. One hour after the embolization, the nylon suture was pulled out ligating the ECA and opening the ICA and CCA. In the sham operation group, a nylon suture was inserted at 5 mm depth to simulate the above procedure. The animal experiments were performed in accordance with the Guidelines for the Care and Use of Laboratory Animals and approved by the Animal Ethics Committee in Affiliated Hospital of Nanjing University of Traditional Chinese Medicine, Nanjing, China (approval No. 2021 DW-09-02)

## Neurological evaluation

After 24 h of modeling, a neurological evaluation of the rats in each group was performed; the examiner was blinded according to the Bederson's method.<sup>34</sup> The rats were suspended 1 m above the ground by gently holding their tails, and the bending of their forelimbs was observed. Rats with forelimbs bilaterally extended

to the floor and no other neurological defects were given a score of 0. Rats with any amount of consistent forelimb flexion and no other abnormality received a score of 1. The rats were then placed on a large sheet of soft plastic paper which they held onto tightly with their claws. The tail of each rat was held and a slight lateral pressure was applied from behind the rat's shoulder until the forelimb slid a few inches. This was repeated several times in each direction. Normal or slightly dysfunctional rats had equal sliding resistance in both directions. However, severely dysfunctional rats had a consistently reduced resistance to the lateral push toward the paretic side and received a score of 2. Next, the rats were allowed to move freely and their circling behavior was observed. Rats that circled to the paralytic side received a score of 3. These experiments were repeated 3 times.

## Hematoxylin and eosin staining

After 24 h of modeling, the rats were euthanized by an injection of excessive anesthetic, and their hippocampal tissue was stripped. The hippocampal tissue was fixed using 10% paraformaldehyde for 24 h, dehydrated with increasing gradients of ethanol (50%, 70%, 85%, 95%, 100%), cleared with xylene for 2 h, embedded in paraffin, and 4-μm sections were obtained. The sections were then soaked in 100%, 95%, 85%, and 75% ethanol solutions for 5 min each, washed with distilled water for 5 min, stained with 2% hematoxylin for 5 min, stained with 0.5% eosin for 2 min, washed with distilled water for 30 s, soaked in 80% ethanol for 30 s, soaked in 95% ethanol for 2 min, soaked in absolute ethanol for 3 min, cleared for 3 min using xylene, and then sealed with neutral resin. The hippocampal tissue sections were observed using a light microscope (model BX41; Olympus Corp., Tokyo, Japan). Each experiment was repeated 3 times.

## TUNEL staining

After dewaxing, the sections were treated in an oven at 65°C for 30 min, soaked in xylene for 10 min, and then soaked in decreasing gradients of ethanol (100%, 95%, 90%, 80%, 70%) for 3 min. The sections were treated with protease K for 30 min and then with 3% H<sub>2</sub>O<sub>2</sub> for 10 min at room

temperature in the dark. After cleaning with phosphate-buffered saline (PBS) for 5 min, sections were incubated in a terminal deoxynucleotidyl transferase (TdT) enzyme buffer for 5 min and then placed in a wet box of TdT reaction solution at 37°C for 1 h. The reaction was then terminated using a termination reaction buffer. The 3,3'-diaminobenzidine (DAB) was used for visualization at room temperature for 10 min. The sections were then counterstained with hematoxylin at room temperature. The number of terminal deoxynucleotidyl transferase dUTP nick end labeling (TUNEL)-positive cells (brownish yellow) was measured using an light microscope (BX41; Olympus Corp.). The experiment was repeated 3 times.

## Brain water content

At 24 h after reperfusion, the brains of the rats were collected after euthanasia and immediately weighed to obtain the wet weight. The brains were then put in an oven (100°C) for 72 h and weighed to obtain the dry weight. The brain water content was calculated using the following formula: (wet weight–dry weight)/wet weight  $\times$  100%. The experiment was repeated 3 times.

## Immunofluorescence

The sections were heated at 65°C for 30 min in a microwave oven, dehydrated with xylene and ethanol, and then antigen repairing was performed using a microwave. After blocking with bovine serum albumin (BSA), LC3 and p62, antibodies were added to the sections and incubated overnight at 4°C. After rinsing, fluorescent-labeled secondary antibodies were added, 4',6-diamidino-2-phenylindole (DAPI) was added to stain the nucleus, and an anti-fluorescence quenching agent was added to seal the sections. The results were observed using a Leica TCS SP5 microscope (Leica Microsystems, Wetzlar, Germany). The experiment was repeated 3 times.

The cells were fixed with 4% paraformaldehyde for 15 min, then pretreated with 0.5% Triton X-100 at room temperature for 20 min, sealed with goat serum for 30 min at room temperature, incubated overnight with the corresponding primary antibody in a wet box at 4°C, and incubated with the corresponding secondary antibody for 1 h in the dark at room temperature. Nuclear counterstaining was performed by incubating the sections with DAPI in the dark for 5 min. The sections were then sealed with an anti-fluorescence quenching agent, and the results were observed using a Leica TCS SP5 microscope (Leica Microsystems). The experiment was repeated 3 times.

## Western blot

Hippocampal tissues and cells were lysed using radio-immunoprecipitation assay (RIPA) lysate containing phenylmethylsulfonyl fluoride (PMSF; Beyotime, Shanghai,

China), and proteins were obtained by centrifugation at 12,000 g for 15 min at 4°C. The protein content was identified using a BCA detection kit (Beyotime). For each group, 30  $\mu$ g of protein were separated on a 10% sodium dodecyl-sulfate polyacrylamide gel electrophoresis (SDS-PAGE) background and then blotted onto a polyvinylidene difluoride (PVDF) membrane. The membranes were blocked for 1 h using 5% skimmed milk powder at room temperature and then incubated with the corresponding primary antibody overnight at 4°C. Then, the membranes were incubated with the corresponding secondary antibody for 2 h at room temperature. ImageJ software (National Institutes of Health, Bethesda, USA; <https://imagej.nih.gov/ij/download.html>) was used to quantify the protein bands, and glyceraldehyde-3-phosphate dehydrogenase (GAPDH) was used as an internal control. The experiment was repeated 3 times.

## Cell culture and group

Mouse hippocampal neuron cell line HT22 cells were obtained from the China Center for Type Culture Collection at Wuhan University, Wuhan, China. The HT22 cells were cultured in a Dulbecco's modified Eagle's medium (DMEM) containing 10% fetal bovine serum (FBS) and 5% CO<sub>2</sub> in an incubator at 37°C. The HT22 cells were then inoculated into 24-well plates at a concentration of  $1 \times 10^5$ /mL. The cells were randomly divided into a control group, OGD/R group, SS-L group, SS-M group, and SS-H group. The cells were pretreated with SS (at concentrations of 0.1  $\mu$ M, 0.5  $\mu$ M and 1  $\mu$ M)<sup>35</sup> for 24 h before OGD/R. After 24 h of culturing, the cells in the OGD/R group and SS treatment groups were cultured in DMEM without glucose in a medium containing 95% N<sub>2</sub>/5% CO<sub>2</sub> at 37°C. After 4 h, the cells were again incubated in DMEM with glucose and returned to the conditions of 95% air/5% CO<sub>2</sub> for 24 h at 37°C. The cells in the control group were incubated in the culture conditions as described above.

## CCK-8

The cells were inoculated into the 96-well plates using a concentration of  $8 \times 10^4$ /mL. After culturing for 24 h, the medium was discarded and 110  $\mu$ L of complete medium containing 10% Cell Counting Kit-8 (CCK-8) (Beyotime) were added to each well. The cells were incubated for 2 h at 37°C. Next, the absorbance value at 450 nm was measured using a microplate reader (Bio-Rad, Hercules, USA). The experiment was repeated 3 times.

## Flow cytometry

The cells were collected and fixed overnight at 4°C using precooled 75% ethanol. The ethanol was then removed by centrifugation (1000 rpm, 5 min), and the cells were washed 3 times using PBS. The cells were then mixed with



5  $\mu$ L of Annexin V/FITC and 10  $\mu$ L of propidium iodide solution (20  $\mu$ g/mL), and the degree of apoptosis was measured using a BD FACSCalibur™ Flow Cytometer (BD Biosciences, Franklin Lakes, USA) within 1 h of adding the mixture. The experiment was repeated 3 times.

## ELISA

After adjusting the cell concentration to  $8 \times 10^4$ /mL, the cells were inoculated onto 96-well plates and cultured at 37°C for 24 h in a 5% CO<sub>2</sub> incubator. After the treatment of the cell as previously described, the cell supernatant was collected using centrifugation at 5000 rpm for 10 min. The amount of interleukin (IL)-1 $\beta$ , tumor necrosis factor alpha (TNF- $\alpha$ ) and IL-6 was measured according to the instructions of the corresponding kit (Nanjing Jiancheng Bioengineering Institute, Nanjing, China). The experiment was repeated 3 times.

The animal serum was separated using centrifugation at 3000 rpm for 10 min. The amount of IL-1 $\beta$ , TNF- $\alpha$  and IL-6 in the serum of each group was detected according to the instructions to the corresponding kit. The experiment was repeated 3 times.

## Statistical analyses

The data from each group were analyzed statistically using GraphPad Prism v. 5.0 (GraphPad Software, San Diego, USA). The measurement data were reported as the mean  $\pm$  standard deviation ( $\bar{x} \pm SD$ ). The normality of the distribution was tested using the Shapiro–Wilk test. Since all the distributions were normal, the Brown–Forsythe test was used to establish the equality of variances, and then significant differences between multiple groups were analyzed using a one-way analysis of variance (ANOVA), followed by Tukey’s post hoc test. When the test standard had a value of  $p < 0.05$ , the difference was considered statistically significant. The results of the assumptions of the verifying tests and the results of the analyses are presented in the Supplementary Table (<https://doi.org/10.5281/zenodo.6838287>).

## Results

### SS treatment alleviated CI/RI and reduced apoptosis and inflammation in MCAO rats

The ability of SS to alleviate CI/RI was investigated in rats. The results of hematoxylin and eosin (H&E) staining showed that compared to the sham group, the MCAO group exhibited obvious interstitial edema, brain tissue structure disorder, partial cell necrosis, and increased inflammatory cell infiltration (Fig. 1A). However, compared to the MCAO group, the degree of brain tissue necrosis was reduced, cell structure was maintained, interstitial

edema was mild, and inflammation was reduced in the SS treatment groups, and the improvement effect was dose-dependent (Fig. 1A). Compared to the sham group, the neurological score of the MCAO group significantly increased ( $p < 0.05$ ; Fig. 1B). However, the treatment with SS effectively alleviated the MCAO-induced neurological deficit observed in the rats ( $p < 0.05$ ; Fig. 1B). The brain edema seen in the MCAO group was more serious than in the sham group ( $p < 0.05$ ), and the administration of SS significantly reduced the brain edema observed in MCAO rats ( $p < 0.05$ ; Fig. 1C). The effects of SS on apoptosis and inflammation were explored in MCAO rats. The results of the TUNEL assay indicated that MCAO increased the number of apoptosis-positive cells in the hippocampus, and SS inhibited the MCAO-induced apoptosis (Fig. 1D). The results of the enzyme-linked immunosorbent assay (ELISA) assay showed that MCAO upregulated the amount of the inflammatory factors IL-1 $\beta$ , TNF- $\alpha$  and IL-6 in rat serum ( $p < 0.05$ ). The treatment using SS reduced the levels of the inflammatory factors ( $p < 0.05$ , Fig. 1E,G). Therefore, SS treatment protected against CI/RI in MCAO rats.

### SS enhanced autophagy and regulated the AMPK/mTOR pathway in MCAO rats

To evaluate the role of SS in the regulation of autophagy during CI/RI, the expression of autophagy markers LC3 and p62 was detected with immunofluorescence staining and western blot. The expression of LC3 in the hippocampus was increased by the MCAO, while the expression of p62 was decreased (Fig. 2A). The expression of LC3 was further enhanced and the expression of p62 was further decreased after SS treatment (Fig. 2A). In addition, MCAO also increased the LC3II/LC3I ratio and decreased p62 levels ( $p < 0.05$ ). Similarly, the administration of SS further promoted the effects of the MCAO on the LC3II/LC3I ratio and the expression of p62 ( $p < 0.05$ , Fig. 2B–D). The AMPK/mTOR pathway plays an important role in the regulation of CI/RI.<sup>36</sup> Next, the regulatory effects of SS on the AMPK/mTOR pathway were assessed in the MCAO rats. Middle cerebral artery occlusion stimulated an increase in the p-AMPK/AMPK ratio and decreased the p-mTOR/mTOR ratio ( $p < 0.05$ , Fig. 2B,E,F). The above effects were significantly increased by SS treatment ( $p < 0.05$ , Fig. 2B,E,F). Therefore, SS enhanced autophagy and regulated the AMPK/mTOR pathway in MCAO rats.

### SS attenuated OGD/R-induced HT22 cell injury

The effects of SS on OGD/R-induced HT22 injury were explored. Schaftoside ( $\leq 1 \mu$ M) was not cytotoxic to HT22 cells ( $p < 0.05$ , Fig. 3A). Our results showed that OGD/R reduced the viability of HT22 cells, and pretreatment with SS weakened this effect ( $p < 0.05$ , Fig. 3B). In addition, SS

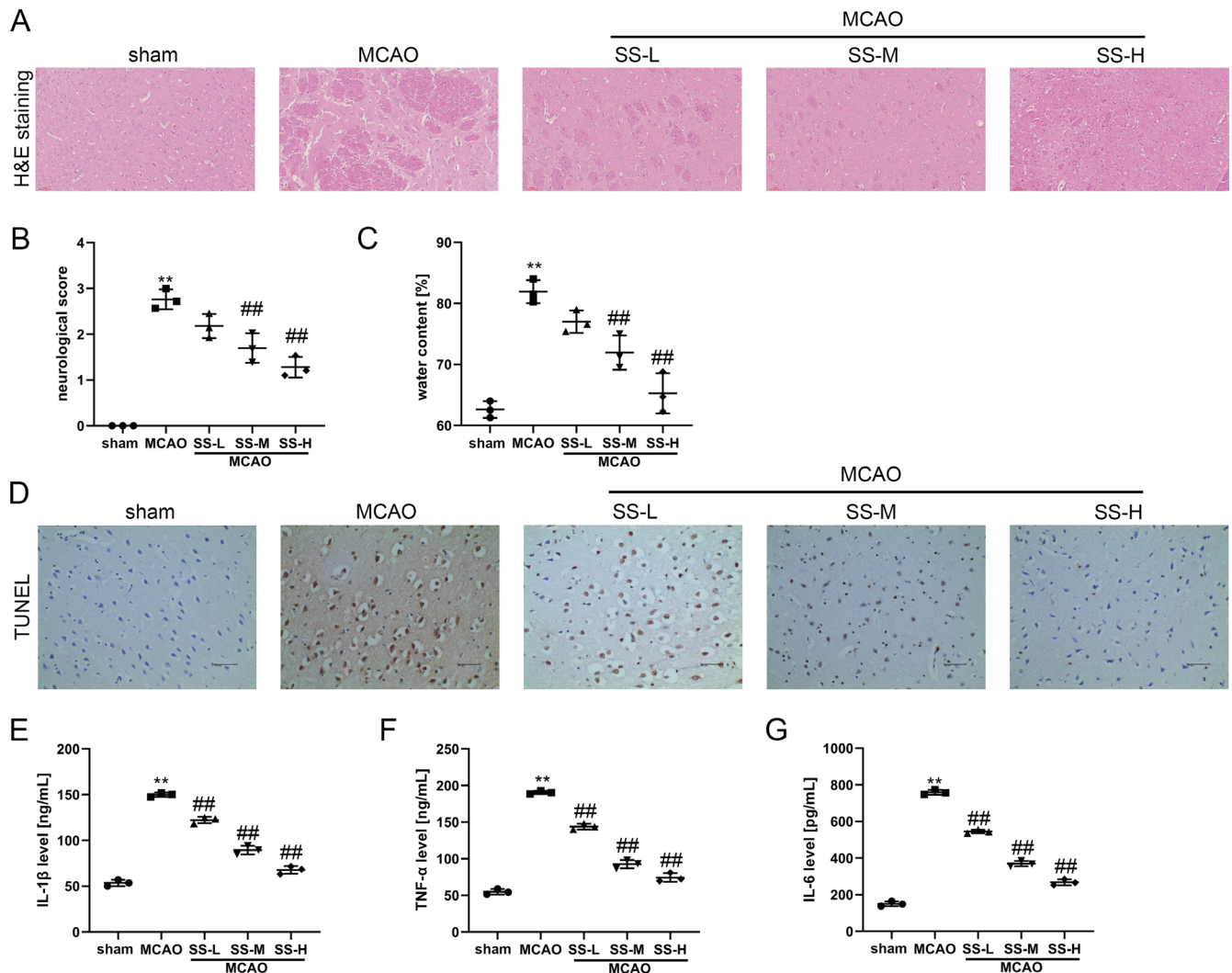


**Fig. 1.** Schaftoside (SS) protected against cerebral ischemia-reperfusion injury (CI/RI) and reduced apoptosis and inflammation. A. Hematoxylin and eosin (H&E) staining was performed on hippocampal tissue; B. Neurological evaluation of rats. The examiner was blinded according to the Bederson's method; C. Calculation of brain water content; D. Evaluation of apoptosis in hippocampal tissue using the terminal deoxynucleotidyl transferase dUTP nick end labeling (TUNEL) assay; E–G. Measurement of inflammation factors (interleukin (IL)-1 $\beta$ , tumor necrosis factor alpha (TNF- $\alpha$ ) and IL-6) using enzyme-linked immunosorbent assay (ELISA)

SS-L – schaftoside low-dose group; SS-M – schaftoside medium-dose group; SS-H – schaftoside high-dose group; \*\* $p < 0.01$  compared to sham group; ## $p < 0.01$  compared to the MCAO group.

treatment significantly alleviated OGD/R-induced apoptosis and inflammation in HT22 cells ( $p < 0.05$ , Fig. 3C–G). Besides, the immunofluorescence results illustrated that SS enhances OGD/R-induced autophagy in HT22 cells, which was demonstrated by the upregulation of LC3 levels (Fig. 4A). Moreover, after HT22 cells underwent OGD/R, the ratio of LC3II/LC3I was markedly increased ( $p < 0.05$ ), while the expression of p62 was reduced ( $p < 0.05$ , Fig. 4B–D). The SS-induced LC3II/LC3I ratio was higher and the p62 level was lower than those in the OGD/R group ( $p < 0.05$ , Fig. 4B–D). Besides, SS treatment enhanced the p-AMPK/AMPK ratio and weakened the p-mTOR/mTOR ratio in OGD/R-induced HT22 cells ( $p < 0.05$ , Fig. 4B,E,F). These findings suggest that SS can reduce OGD/R-induced HT22 cell injury, and the AMPK/mTOR pathway may participate in the effects of SS on CI/RI.

### SS improved the growth of HT22 cells by activating the AMPK/mTOR pathway

The mechanism of SS protection of HT22 cells was explored. To further determine the role of the AMPK/mTOR pathway in HT22 cells against OGD/R, the AMPK inhibitor compound C and mTOR inhibitor rapamycin were used. Schaftoside-induced inhibition of apoptosis and inflammation in HT22 cells against OGD/R were enhanced by rapamycin and blocked by compound C ( $p < 0.05$ , Fig. 5A–D). Rapamycin amplified SS-induced autophagy by reducing the LC3II/LC3I and p-mTOR/mTOR ratios, and upregulating p62 levels ( $p < 0.05$ ). However, compound C showed the opposite effect ( $p < 0.05$ , Fig. 5F–J). Therefore, SS prevented HT22 cell injury induced by OGD/R by activating the AMPK/mTOR pathway.

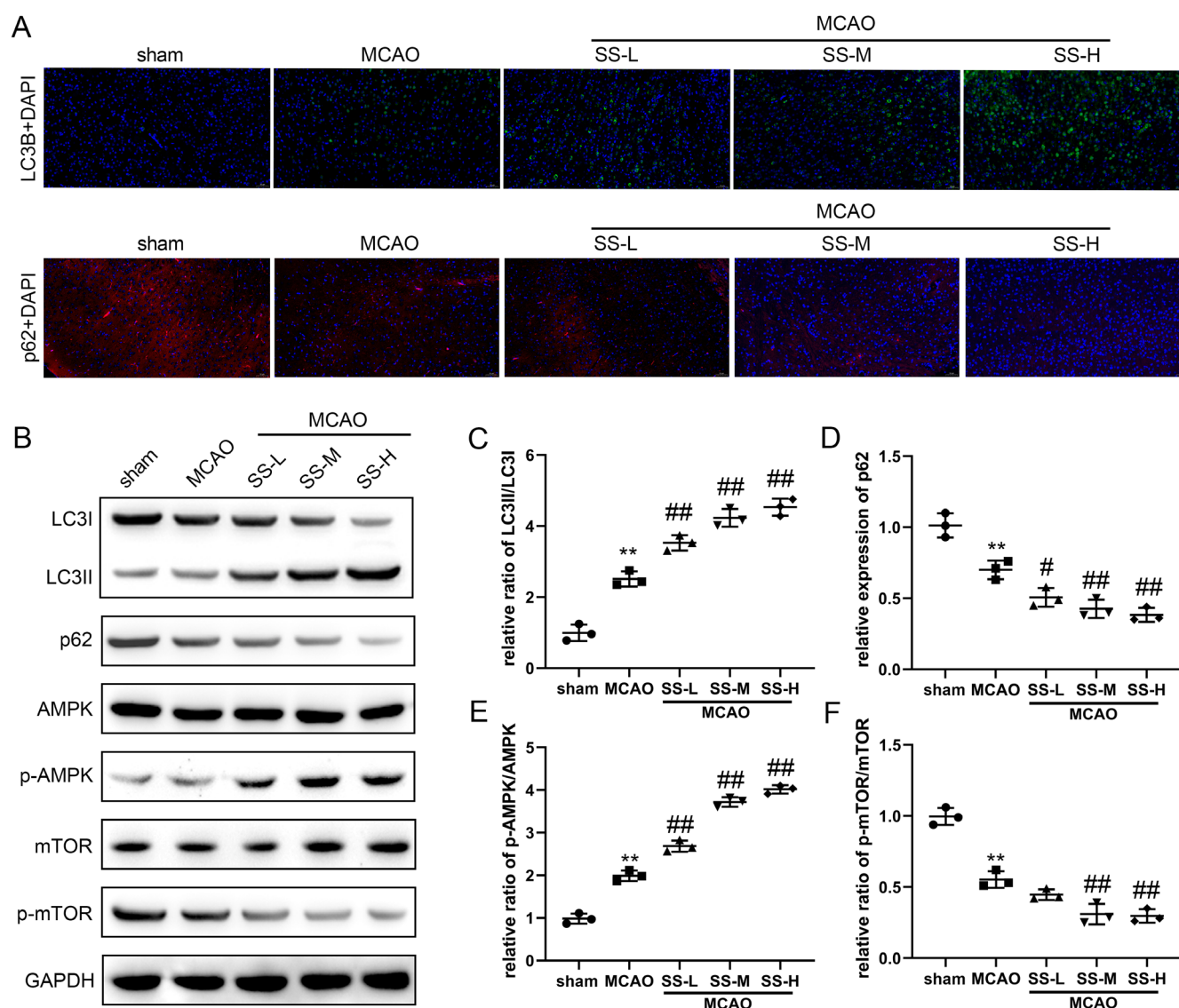


**Fig. 2.** Schaftoside (SS) promoted autophagy and activated the adenosine monophosphate-activated protein kinase (AMPK)/mammalian target of rapamycin (mTOR) pathway in middle cerebral artery occlusion (MCAO) rats. A. The expression of LC3 and p62 was detected with immunofluorescence assay; B–F. Related proteins of autophagy (LC3, p62) and the AMPK/mTOR pathway (AMPK, p-AMPK, mTOR, p-mTOR) were assessed using western blot

SS-L – schaftoside low-dose group; SS-M – schaftoside medium-dose group; SS-H – schaftoside high-dose group; DAPI – 4',6-diamidino-2-phenylindole; GAPDH – glyceraldehyde-3-phosphate dehydrogenase; \*\* $p < 0.01$  compared to the sham group; # $p < 0.05$  compared to the MCAO group; ## $p < 0.01$  compared to the MCAO group.

## Discussion

Stroke is the leading cause of death and neurological dysfunction and places a heavy financial burden on the victims and health systems around the world. Previous studies have confirmed that CI/RI can lead to vascular injury, blood–brain barrier damage and a series of effects on neuronal injury. However, there is still a lot of work to be done to reduce the adverse effects of CI/RI. Despite continuous efforts to develop new treatment strategies (such as noninvasive brain stimulation techniques (NIBS)<sup>37–39</sup>), there are no effective treatment schemes for CI/RI. This study explored the potential neuroprotective effects of SS on brain I/R injuries and its mechanism.

Middle cerebral artery occlusion is a stable animal model for focal transient cerebral ischemia which is similar to human cerebral ischemia.<sup>40</sup> Therefore, MCAO is widely used in research on stroke pathology and neuroprotective drug screenings.<sup>41</sup> Neuronal death caused by CI/RI can lead to serious neurological deficits and cognitive impairments. After ischemia, the nutritional supply to neurons is blocked, including oxygen and glucose which play an important role in the growth of neurons.<sup>42</sup> Therefore, OGD/R-induced neuronal injury is used to simulate CI/RI in vitro.<sup>43</sup> In our study, we explored the effects of SS on CI/RI through an in vivo model of MCAO rats and the in vitro model of OGD/R-induced HT22 cells. Our findings suggested that SS reduced neuronal apoptosis and inflammation and

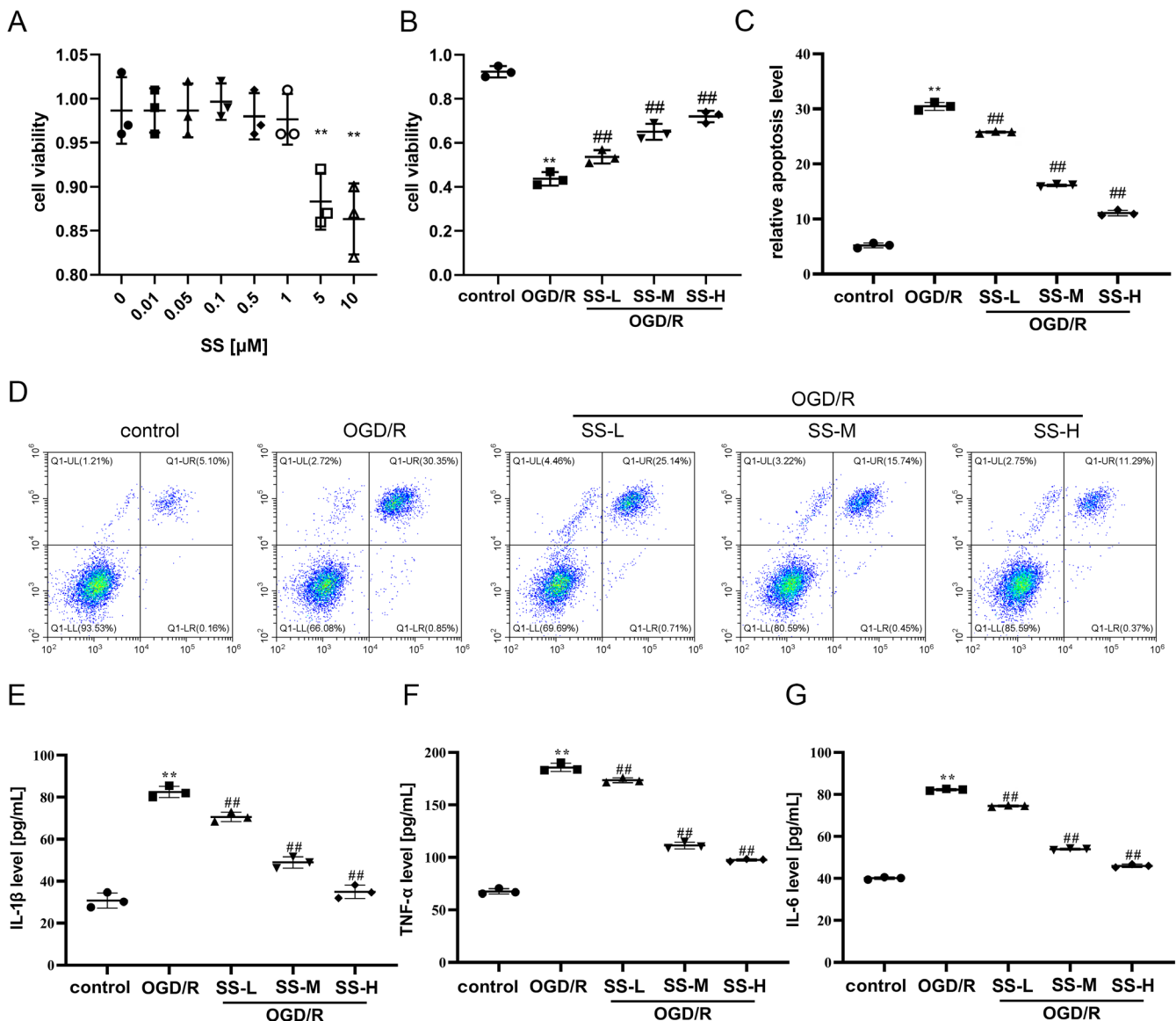


Fig. 3. Schaftoside (SS) increased cell viability and reduced apoptosis and inflammation in oxygen glucose deprivation/reperfusion (OGD/R)-induced HT22 cells. A,B. The cell viability was evaluated using the Cell Counting Kit-8 (CCK-8) assay; C,D. Cell apoptosis was measured using flow cytometry; E–G. Inflammation factors (interleukin (IL)-1 $\beta$ , tumor necrosis factor alpha (TNF- $\alpha$ ) and IL-6) were measured using enzyme-linked immunosorbent assay (ELISA)

SS-L – schaftoside low-dose group; SS-M – schaftoside medium-dose group; SS-H – schaftoside high-dose group; \*\*p < 0.01 compared to the control group; ##p < 0.01 compared to the OGD/R group.

promoted autophagy in MCAO rats and OGD/R-induced HT22 cells, and its action was related to the activation of the AMPK/mTOR signaling pathway.

Apoptosis, also known as programmed cell death, is a process leading to cell death triggered by internal and external factors.<sup>44</sup> In recent years, scholars have found that CI/RI is closely related to apoptosis.<sup>45,46</sup> In addition, previous studies have confirmed that CI/RI causes inflammation, and reducing neuroinflammation is considered to be an important strategy to prevent CI/RI.<sup>47,48</sup> The upregulation of TREM2 can alleviate neurological dysfunction by inhibiting the inflammatory response and neuronal apoptosis in MCAO mice.<sup>49</sup> It was found that magnolol reduced the production of inflammatory factors and the expression and secretion

of normal T cells in rats, and reduced brain injury in a rat I/R model.<sup>50</sup> Sappanone A effectively mitigated pathologic injury following cerebral infarction by reducing inflammation, oxidative stress and apoptosis in MCAO rats and OGD/R-induced PC12 cells.<sup>51</sup> Stigmasterol inhibits inflammation by regulating cyclooxygenase-2 (COX-2) and NF- $\kappa$ B (p65) expression and attenuates apoptosis by increasing the Bcl-2/Bax ratio and decreasing cleaved caspase-3 levels in rats with CI/RI.<sup>52</sup> Similarly, our results indicate that SS can inhibit apoptosis and inflammation in MCAO rats and OGD/R-induced HT22 cells.

Autophagy is a complex cellular metabolic process.<sup>53</sup> It is used as a metabolic self-defense process that differs from necrosis and apoptosis.<sup>54</sup> Autophagy is a complex



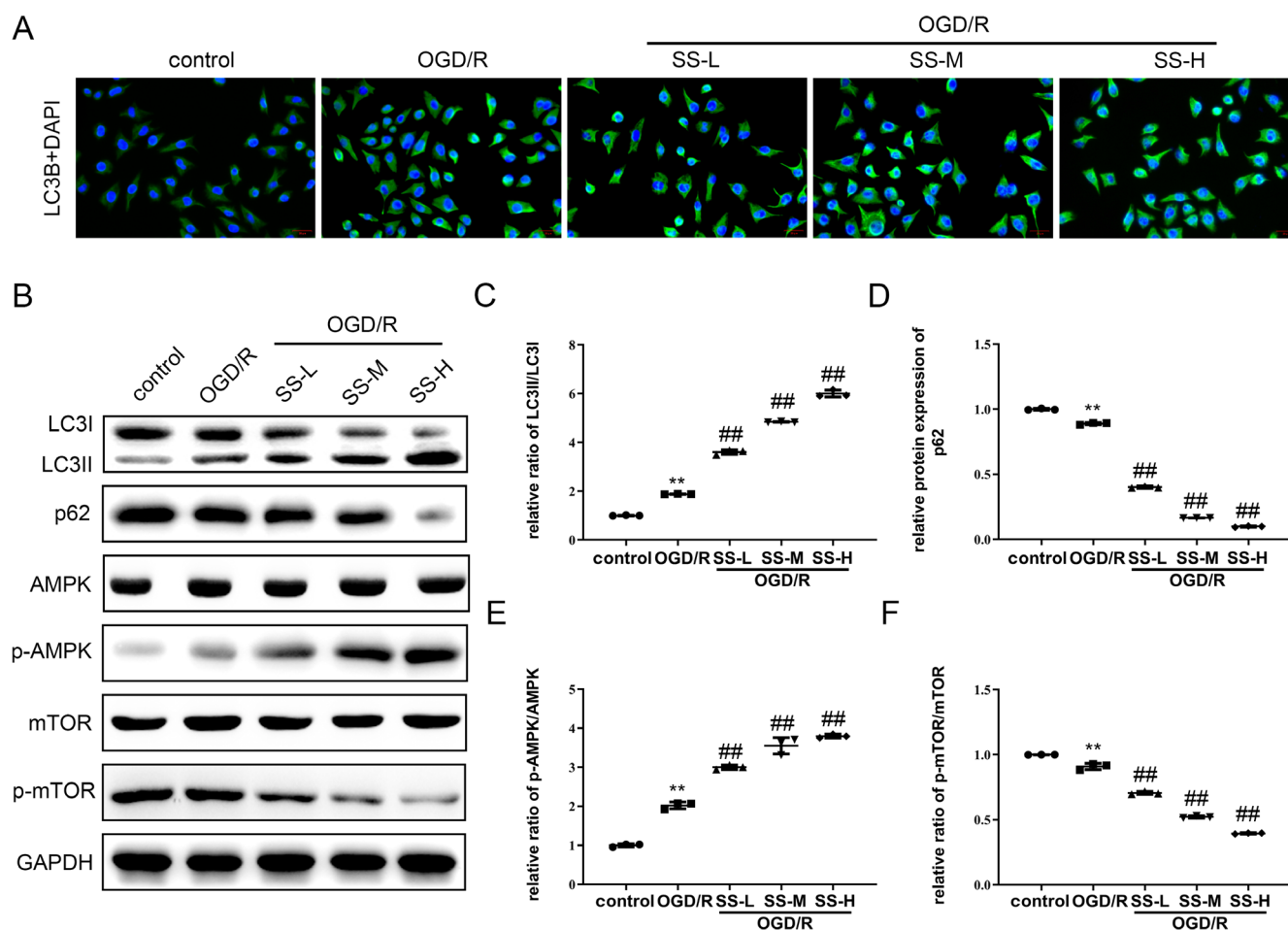


**Fig. 4.** Schaftoside (SS)-enhanced autophagy and activation of the adenosine monophosphate-activated protein kinase (AMPK)/mammalian target of rapamycin (mTOR) pathway in oxygen glucose deprivation/reperfusion (OGD/R)-induced HT22 cells. A. The expression of LC3 was measured with immunofluorescence assay; B–F. Related proteins of autophagy (LC3, p62) and the AMPK/mTOR pathway (AMPK, p-AMPK, mTOR, p-mTOR) were assessed using western blot

SS-L – schaftoside low-dose group; SS-M – schaftoside medium-dose group; SS-H – schaftoside high-dose group; DAPI – 4',6-diamidino-2-phenylindole; GAPDH – glyceraldehyde-3-phosphate dehydrogenase; \*\* $p < 0.01$  compared to the control group; ## $p < 0.01$  compared to the OGD/R group.

dynamic reaction, in which LC3 plays a significant role.<sup>55</sup> The transformation of LC3I to LC3II is considered to be a marker of autophagy.<sup>56</sup> The p62, as the substrate of autophagy, combines with LC3 and is degraded through a lysosomal pathway. It also plays a role in regulating autophagy.<sup>57</sup> Some scholars believe that autophagy plays a neuroprotective role in CI/RI.<sup>58</sup> Resveratrol inhibited the expression of NLRP3 proteins and their downstream inflammatory factors by activating the SIRT-autophagy pathway, and played a protective role in CI/RI.<sup>59</sup> Ibrutinib reduced cerebral infarction volume, alleviated neurological impairment and CI/RI, and promoted autophagy by activating the PI3K/AKT/mTOR pathway in diabetic mice.<sup>60</sup> The results of our study confirmed that SS increases the LC3II/LC3I ratio and decreases p62 expression in MCAO rats and OGD/R-induced HT22 cells, which suggests an increase in autophagic flux.

To study the molecular mechanism of SS in CI/RI, the AMPK/mTOR signaling pathway was evaluated. The AMPK is a serine/threonine protein kinase which is a key energy sensor

to maintain metabolic homeostasis and has been proven to induce the activation of autophagy.<sup>61,62</sup> The mTOR is an important signaling molecule downstream from AMPK that plays a negative regulatory role in autophagy.<sup>63,64</sup> Eugenol enhanced autophagy via regulation of the AMPK/mTOR pathway, and inhibited apoptosis in MCAO rats and OGD/R-induced HT22 cells.<sup>65</sup> Remote limb biochemical postconditioning (RLPoC) played a neuroprotective role by activating the AMPK signaling pathway to induce autophagy.<sup>66</sup> These studies have confirmed that the AMPK/mTOR signaling pathway is also involved in the regulation of inflammation and apoptosis.<sup>67,68</sup> Tissue-type plasminogen activator (tPA) exerted neuroprotective effects by increasing the phosphorylation of AMPK, thereby inhibiting apoptosis and improving mitochondrial function.<sup>69</sup> Dexmedetomidine improved neuroinflammation in rats by activating the AMPK signaling pathway.<sup>70</sup> In our study, the phosphorylation of AMPK was enhanced and the phosphorylation of mTOR was reduced in MCAO rats and OGD/R-induced HT22 cells, which was amplified by SS. Compound C (AMPK inhibitor) and rapamycin (mTOR

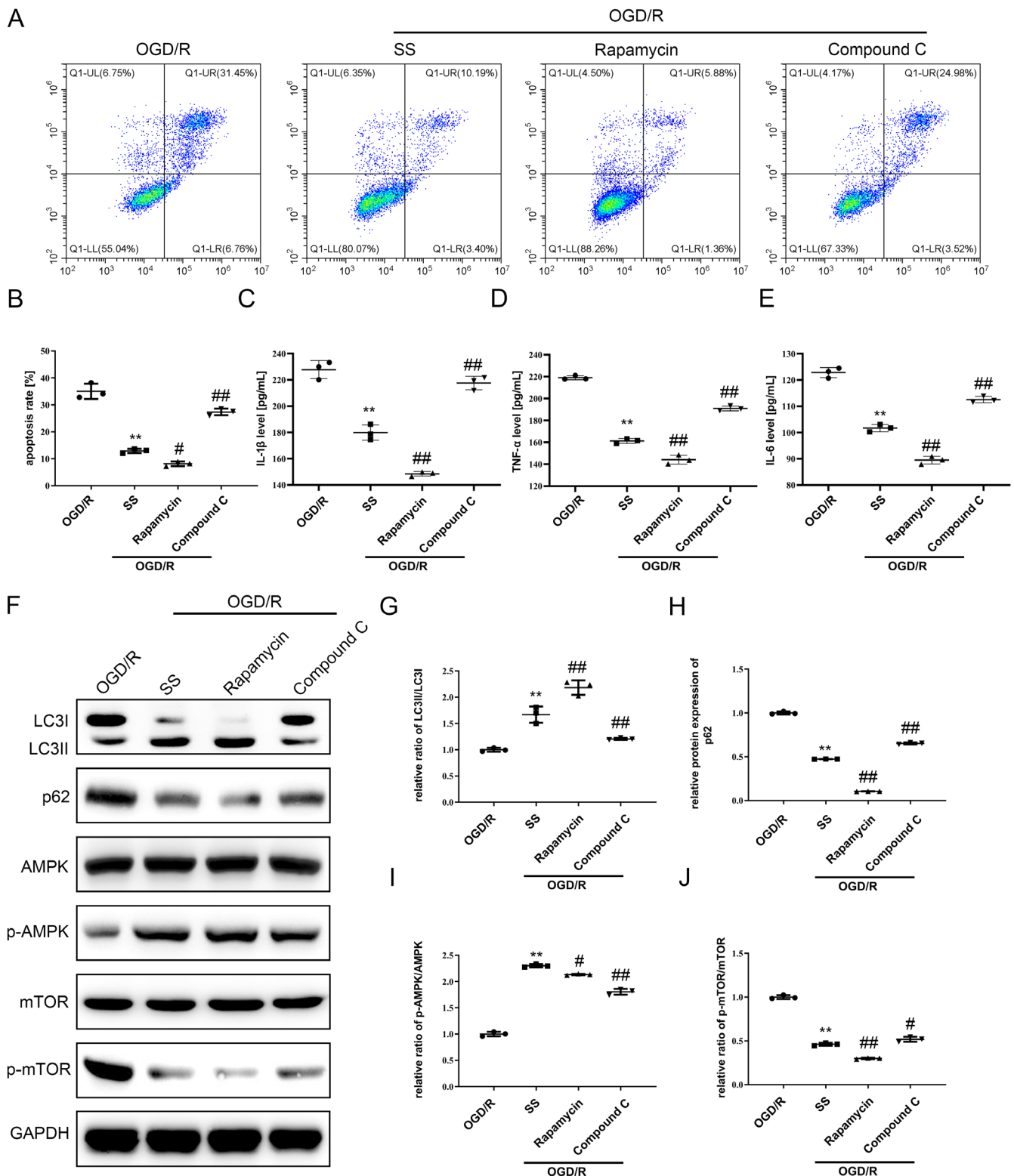


**Fig. 5.** Schaftoside (SS)-amplified autophagy and reduced apoptosis and inflammation through the regulation of the adenosine monophosphate-activated protein kinase (AMPK)/mammalian target of rapamycin (mTOR) pathway in oxygen glucose deprivation/reperfusion (OGD/R)-induced HT22 cells. A,B. Cell apoptosis was measured using flow cytometry; C–E. Inflammation factors (interleukin (IL)-1 $\beta$ , tumor necrosis factor alpha (TNF- $\alpha$ ) and IL-6) were measured using enzyme-linked immunosorbent assay (ELISA); F–J. Related proteins of autophagy (LC3, p62) and the AMPK/mTOR pathway (AMPK, p-AMPK, mTOR, p-mTOR) were assessed with western blot

GAPDH – glyceraldehyde-3-phosphate dehydrogenase; \*\* $p < 0.01$  compared to the OGD/R group; # $p < 0.05$  compared to the SS+OGD/R group; ## $p < 0.01$  compared to the SS+OGD/R group.

inhibitor) were used in our study. Our previous studies have demonstrated that SS reduced apoptosis and inflammation and promoted autophagy to resist CI/RI. Our results further confirmed that rapamycin enhances the protective effects of SS in CI/RI, but compound C reverses the beneficial effects of SS in CI/RI.

## Limitations

There are some limitations in our study. Although we evaluated the protective effect of pretreatment with SS in CI/RI, the time window of the protective effects of SS needs to be investigated. In addition, whether SS could reduce CI/RI through the regulation of other signaling pathways requires further research.

## Conclusions


Our study demonstrated that SS protected against CI/RI by inhibiting apoptosis and inflammation and promoting the activation of autophagy. The protective role of SS in CI/RI may be a result of the activation of the AMPK/mTOR signaling pathway. Our findings provide better insight into the function of SS in CI/RI, which could contribute to the clinical treatment of stroke.


## Supplementary files

The data concerning verification of assumptions for the application of the ANOVA through ANOVA test and post hoc test with p-values are available at <https://doi.org/10.5281/zenodo.6838287>.

## ORCID IDs

Lin Zhang  <https://orcid.org/0000-0002-0075-027X>

Minghua Wu  <https://orcid.org/0000-0003-2855-2301>

Zhaoyao Chen  <https://orcid.org/0000-0002-8441-5355>

## References

- Guzik A, Bushnell C. Stroke epidemiology and risk factor management. *Continuum (Minneapolis Minn)*. 2017;23(1):15–39. doi:10.1212/CON.0000000000000416
- Toman NG, Grande AW, Low WC. Neural repair in stroke. *Cell Transplant*. 2019;28(9–10):1123–1126. doi:10.1177/0963689719863784
- Unnithan AKA, Das J, Mehta P. Hemorrhagic stroke. In: *StatPearls*. Treasure Island, USA: StatPearls Publishing; 2022. <http://www.ncbi.nlm.nih.gov/books/NBK559173/>. Accessed August 8, 2022.
- Kim J, Thayabaranathan T, Donnan GA, et al. Global Stroke Statistics 2019. *Int J Stroke*. 2020;15(8):819–838. doi:10.1177/1747493020909545
- Caprio FZ, Sorond FA. Cerebrovascular disease: Primary and secondary stroke prevention. *Med Clin North Am*. 2019;103(2):295–308. doi:10.1016/j.mcna.2018.10.001
- Mair G, Wardlaw JM. Imaging of acute stroke prior to treatment: Current practice and evolving techniques. *Br J Radiol*. 2014;87(1040):20140216. doi:10.1259/bjr.20140216
- Cramer SC. Recovery after stroke. *Continuum (Minneapolis Minn)*. 2020;26(2):415–434. doi:10.1212/CON.0000000000000838
- Wardlaw JM, Murray V, Berge E, del Zoppo GJ. Thrombolysis for acute ischaemic stroke. *Cochrane Database Syst Rev*. 2014;2014(7):CD000213. doi:10.1002/14651858.CD000213.pub3
- Liu R, Li H, Deng J, et al. QKI 6 ameliorates CIRI through promoting synthesis of triglyceride in neuron and inhibiting neuronal apoptosis associated with SIRT1-PPAR $\gamma$ -PGC-1 $\alpha$  axis. *Brain Behav*. 2021;11(8):e2271. doi:10.1002/brb3.2271
- Battaglia S, Garofalo S, di Pellegrino G, Starita F. Revaluing the role of vmPFC in the acquisition of Pavlovian threat conditioning in humans. *J Neurosci*. 2020;40(44):8491–8500. doi:10.1523/JNEUROSCI.0304-20.2020
- Battaglia S. Neurobiological advances of learned fear in humans. *Adv Clin Exp Med*. 2022;31(3):217–221. doi:10.17219/acem/146756
- Battaglia S, Fabius JH, Moravkova K, Fracasso A, Borgomaneri S. The neurobiological correlates of gaze perception in healthy individuals and neurologic patients. *Biomedicine*. 2022;10(3):627. doi:10.3390/biomedicine10030627
- Xu J, Kong X, Xiu H, Dou Y, Wu Z, Sun P. Combination of curcumin and vagus nerve stimulation attenuates cerebral ischemia/reperfusion injury-induced behavioral deficits. *Biomed Pharmacother*. 2018;103:614–620. doi:10.1016/j.biopha.2018.04.069
- Shi Y, Yi Z, Zhao P, Xu Y, Pan P. MicroRNA-532-5p protects against cerebral ischemia-reperfusion injury by directly targeting CXCL1. *Aging (Albany NY)*. 2021;13(8):11528–11541. doi:10.18632/aging.202846
- Deng Z, Ou H, Ren F, et al. LncRNA SNHG14 promotes OGD/R-induced neuron injury by inducing excessive mitophagy via miR-182-5p/BINP3 axis in HT22 mouse hippocampal neuronal cells. *Biol Res*. 2020;53(1):38. doi:10.1186/s40659-020-00304-4
- Wu MY, Yang GT, Liao WT, et al. Current mechanistic concepts in ischemia and reperfusion injury. *Cell Physiol Biochem*. 2018;46(4):1650–1667. doi:10.1159/000489241
- Galluzzi L, Green DR. Autophagy-independent functions of the autophagy machinery. *Cell*. 2019;177(7):1682–1699. doi:10.1016/j.cell.2019.05.026
- Mo Y, Sun YY, Liu KY. Autophagy and inflammation in ischemic stroke. *Neural Regen Res*. 2020;15(8):1388–1396. doi:10.4103/1673-5374.274331
- Ahsan A, Liu M, Zheng Y, et al. Natural compounds modulate the autophagy with potential implication of stroke. *Acta Pharm Sin B*. 2021;11(7):1708–1720. doi:10.1016/j.apsb.2020.10.018
- Liu L, Cao Q, Gao W, et al. Melatonin ameliorates cerebral ischemia-reperfusion injury in diabetic mice by enhancing autophagy via the SIRT1-BMAL1 pathway. *FASEB J*. 2021;35(12):e22040. doi:10.1096/fj.202002718RR
- Maiuri MC, Zalckvar E, Kimchi A, Kroemer G. Self-eating and self-killing: Crosstalk between autophagy and apoptosis. *Nat Rev Mol Cell Biol*. 2007;8(9):741–752. doi:10.1038/nrm2239
- Zhang Y, Zhang Y, Jin XF, et al. The role of Astragaloside IV against cerebral ischemia/reperfusion injury: Suppression of apoptosis via promotion of P62-LC3-autophagy. *Molecules*. 2019;24(9):1838. doi:10.3390/molecules24091838
- Tanaka M, Toldi J, Vécsei L. Exploring the etiological links behind neurodegenerative diseases: Inflammatory cytokines and bioactive kynurenines. *Int J Mol Sci*. 2020;21(7):2431. doi:10.3390/ijms21072431
- Lambertsen KL, Finsen B, Clausen BH. Post-stroke inflammation: Target or tool for therapy? *Acta Neuropathol*. 2019;137(5):693–714. doi:10.1007/s00401-018-1930-z
- Chamorro A, Dirnagl U, Urra X, Planas AM. Neuroprotection in acute stroke: Targeting excitotoxicity, oxidative and nitrosative stress, and inflammation. *Lancet Neurol*. 2016;15(8):869–881. doi:10.1016/S1474-4422(16)00114-9
- Ma Y, Zhou K, Fan J, Sun S. Traditional Chinese medicine: Potential approaches from modern dynamical complexity theories. *Front Med*. 2016;10(1):28–32. doi:10.1007/s11684-016-0434-2
- Yang Y, Zhang M, Zhao J, Song S, Hong F, Zhang G. Effect of traditional Chinese medicine emotional therapy on post-stroke depression: A protocol for systematic review and meta-analysis. *Medicine (Baltimore)*. 2021;100(14):e25386. doi:10.1097/MD.00000000000025386
- Gong X, Sucher NJ. Stroke therapy in traditional Chinese medicine (TCM): Prospects for drug discovery and development. *Phytomedicine*. 2002;9(5):478–484. doi:10.1078/0944711026051760
- Liu M, Zhang G, Wu S, et al. Schafostide alleviates HFD-induced hepatic lipid accumulation in mice via upregulating farnesoid X receptor. *J Ethnopharmacol*. 2020;255:112776. doi:10.1016/j.jep.2020.112776
- Kim PS, Shin JH, Jo DS, et al. Anti-melanogenic activity of schafostide in *Rhizoma Arisaematis* by increasing autophagy in B16F1 cells. *Biochem Biophys Res Commun*. 2018;503(1):309–315. doi:10.1016/j.bbrc.2018.06.021

31. Kou X, Chen N. Resveratrol as a natural autophagy regulator for prevention and treatment of Alzheimer's disease. *Nutrients*. 2017;9(9):927. doi:10.3390/nu9090927
32. Yang X, Jiang T, Wang Y, Guo L. The role and mechanism of SIRT1 in resveratrol-regulated osteoblast autophagy in osteoporosis rats. *Sci Rep*. 2019;9(1):18424. doi:10.1038/s41598-019-44766-3
33. Liu R, Meng C, Zhang Z, et al. Comparative metabolism of schaftoside in healthy and calcium oxalate kidney stone rats by UHPLC-Q-TOF-MS/MS method. *Anal Biochem*. 2020;597:113673. doi:10.1016/j.ab.2020.113673
34. Bieber M, Schuhmann MK, Volz J, et al. Description of a novel phosphodiesterase (PDE)-3 inhibitor protecting mice from ischemic stroke independent from platelet function. *Stroke*. 2019;50(2):478–486. doi:10.1161/STROKEAHA.118.023664
35. Zhou K, Wu J, Chen J, et al. Schaftoside ameliorates oxygen glucose deprivation-induced inflammation associated with the TLR4/Myd88/Drp1-related mitochondrial fission in BV2 microglia cells. *J Pharmacol Sci*. 2019;139(1):15–22. doi:10.1016/j.jpshs.2018.10.012
36. Wang G, Wang T, Zhang Y, Li F, Yu B, Kou J. Schizandrin protects against OGD/R-induced neuronal injury by suppressing autophagy: Involvement of the AMPK/mTOR pathway. *Molecules*. 2019;24(19):3624. doi:10.3390/molecules24193624
37. Borgomaneri S, Battaglia S, Garofalo S, Tortora F, Avenanti A, di Pellegrino G. State-dependent TMS over prefrontal cortex disrupts fear-memory reconsolidation and prevents the return of fear. *Curr Biol*. 2020;30(18):3672–3679.e4. doi:10.1016/j.cub.2020.06.091
38. Hara T, Shanmugalingam A, McIntyre A, Burhan AM. The effect of non-invasive brain stimulation (NIBS) on attention and memory function in stroke rehabilitation patients: A systematic review and meta-analysis. *Diagnostics (Basel)*. 2021;11(2):227. doi:10.3390/diagnostics11020227
39. Borgomaneri S, Battaglia S, Sciamanna G, Tortora F, Laricchiuta D. Memories are not written in stone: Re-writing fear memories by means of non-invasive brain stimulation and optogenetic manipulations. *Neurosci Biobehav Rev*. 2021;127:334–352. doi:10.1016/j.neubiorev.2021.04.036
40. Tang H, Gamdzyk M, Huang L, et al. Delayed recanalization after MCAO ameliorates ischemic stroke by inhibiting apoptosis via HGF/c-Met/STAT3/Bcl-2 pathway in rats. *Exp Neurol*. 2020;330:113359. doi:10.1016/j.expneurol.2020.113359
41. Barthels D, Das H. Current advances in ischemic stroke research and therapies. *Biochim Biophys Acta Mol Basis Dis*. 2020;1866(4):165260. doi:10.1016/j.bbadis.2018.09.012
42. Wang Y, Li Y, Ma C, et al. LncRNA XIST promoted OGD-induced neuronal injury through modulating/miR-455-3p/TIPARP axis. *Neurochem Res*. 2021;46(6):1447–1456. doi:10.1007/s11064-021-03286-1
43. Ryou MG, Mallet RT. An in vitro oxygen–glucose deprivation model for studying ischemia-reperfusion injury of neuronal cells. In: Tharakan B, ed. *Traumatic and Ischemic Injury*. Methods in Molecular Biology. New York, USA: Springer New York; 2018:229–235. doi:10.1007/978-1-4939-7526-6\_18
44. Xu X, Lai Y, Hua ZC. Apoptosis and apoptotic body: Disease message and therapeutic target potentials. *Biosci Rep*. 2019;39(1):BSR20180992. doi:10.1042/BSR20180992
45. Gong L, Tang Y, An R, Lin M, Chen L, Du J. RTN1-C mediates cerebral ischemia/reperfusion injury via ER stress and mitochondria-associated apoptosis pathways. *Cell Death Dis*. 2017;8(10):e3080. doi:10.1038/cddis.2017.465
46. Shi C, Jin J, Wang X, et al. Sevoflurane attenuates brain damage through inhibiting autophagy and apoptosis in cerebral ischemia-reperfusion rats. *Mol Med Rep*. 2019;21(1):123–130. doi:10.3892/mmr.2019.10832
47. Franke M, Bieber M, Kraft P, Weber ANR, Stoll G, Schuhmann MK. The NLRP3 inflammasome drives inflammation in ischemia/reperfusion injury after transient middle cerebral artery occlusion in mice. *Brain Behav Immun*. 2021;92:223–233. doi:10.1016/j.bbi.2020.12.009
48. Liu H, Wu X, Luo J, et al. Pterostilbene attenuates astrocytic inflammation and neuronal oxidative injury after ischemia-reperfusion by inhibiting NF- $\kappa$ B phosphorylation. *Front Immunol*. 2019;10:2408. doi:10.3389/fimmu.2019.02408
49. Wu R, Li X, Xu P, et al. TREM2 protects against cerebral ischemia/reperfusion injury. *Mol Brain*. 2017;10(1):20. doi:10.1186/s13041-017-0296-9
50. Huang S, Tai S, Chang C, Tu Y, Chang C, Lee E. Magnolol protects against ischemic-reperfusion brain damage following oxygen-glucose deprivation and transient focal cerebral ischemia. *Int J Mol Med*. 2018;41(4):2252–2262. doi:10.3892/ijmm.2018.3387
51. Wang M, Chen Z, Yang L, Ding L. Sappanone A protects against inflammation, oxidative stress and apoptosis in cerebral ischemia-reperfusion injury by alleviating endoplasmic reticulum stress. *Inflammation*. 2021;44(3):934–945. doi:10.1007/s10753-020-01388-6
52. Liang Q, Yang J, He J, et al. Stigmasterol alleviates cerebral ischemia/reperfusion injury by attenuating inflammation and improving antioxidant defenses in rats. *Biosci Rep*. 2020;40(4):BSR20192133. doi:10.1042/BSR20192133
53. Glick D, Barth S, Macleod KF. Autophagy: Cellular and molecular mechanisms. *J Pathol*. 2010;221(1):3–12. doi:10.1002/path.2697
54. Martínez-Borra J, López-Larrea C. Autophagy and self-defense. In: López-Larrea C, ed. *Self and Nonself*. New York, USA: Springer US; 2012:169–184. doi:10.1007/978-1-4614-1680-7\_11
55. Tanida I, Ueno T, Kominami E. LC3 and autophagy. In: Deretic V, ed. *Autophagosome and Phagosome*. Totowa, USA: Humana Press; 2008:77–88. doi:10.1007/978-1-59745-157-4\_4
56. Runwal G, Stamatakou E, Siddiqi FH, Puri C, Zhu Y, Rubinsztein DC. LC3-positive structures are prominent in autophagy-deficient cells. *Sci Rep*. 2019;9(1):10147. doi:10.1038/s41598-019-46657-z
57. Lamark T, Svenning S, Johansen T. Regulation of selective autophagy: The p62/SQSTM1 paradigm. *Essays Biochem*. 2017;61(6):609–624. doi:10.1042/EBC20170035
58. Huang YG, Tao W, Yang SB, Wang JF, Mei ZG, Feng ZT. Autophagy: Novel insights into therapeutic target of electroacupuncture against cerebral ischemia/reperfusion injury. *Neural Regen Res*. 2019;14(6):954–961. doi:10.4103/1673-5374.250569
59. He Q, Li Z, Wang Y, Hou Y, Li L, Zhao J. Resveratrol alleviates cerebral ischemia/reperfusion injury in rats by inhibiting NLRP3 inflammasome activation through Sirt1-dependent autophagy induction. *Int Immunopharmacol*. 2017;50:208–215. doi:10.1016/j.intimp.2017.06.029
60. Jin L, Mo Y, Yue EL, Liu Y, Liu KY. Ibrutinib ameliorates cerebral ischemia/reperfusion injury through autophagy activation and PI3K/Akt/mTOR signaling pathway in diabetic mice. *Bioengineered*. 2021;12(1):7432–7445. doi:10.1080/21655979.2021.1974810
61. Carling D. AMPK signalling in health and disease. *Curr Opin Cell Biol*. 2017;45:31–37. doi:10.1016/j.cceb.2017.01.005
62. Li Y, Chen Y. AMPK and autophagy. In: Qin ZH, ed. *Autophagy: Biology and Diseases*. Advances in Experimental Medicine and Biology. Singapore: Springer Singapore; 2019:85–108. doi:10.1007/978-981-15-0602-4\_4
63. Inoki K, Kim J, Guan KL. AMPK and mTOR in cellular energy homeostasis and drug targets. *Annu Rev Pharmacol Toxicol*. 2012;52(1):381–400. doi:10.1146/annurev-pharmtox-010611-134537
64. Alers S, Löffler AS, Wesselborg S, Stork B. Role of AMPK-mTOR-Ulk1/2 in the regulation of autophagy: Cross talk, shortcuts, and feedbacks. *Mol Cell Biol*. 2012;32(1):2–11. doi:10.1128/MCB.06159-11
65. Sun X, Wang D, Zhang T, et al. Eugenol attenuates cerebral ischemia-reperfusion injury by enhancing autophagy via AMPK-mTOR-P70S6K pathway. *Front Pharmacol*. 2020;11:84. doi:10.3389/fphar.2020.00084
66. He JT, Li H, Yang L, Cheng KL. Involvement of endothelin-1, H2S and Nrf2 in beneficial effects of remote ischemic preconditioning in global cerebral ischemia-induced vascular dementia in mice. *Cell Mol Neurobiol*. 2019;39(5):671–686. doi:10.1007/s10571-019-00670-y
67. Liu X, Xu Y, Cheng S, et al. Geniposide combined with notoginsenoside R1 attenuates inflammation and apoptosis in atherosclerosis via the AMPK/mTOR/Nrf2 signaling pathway. *Front Pharmacol*. 2021;12:687394. doi:10.3389/fphar.2021.687394
68. Sun Z, Gu L, Wu K, et al. VX-765 enhances autophagy of human umbilical cord mesenchymal stem cells against stroke-induced apoptosis and inflammatory responses via AMPK/mTOR signaling pathway. *CNS Neurosci Ther*. 2020;26(9):952–961. doi:10.1111/cns.13400
69. Cai Y, Yang E, Yao X, et al. FUNDC1-dependent mitophagy induced by tPA protects neurons against cerebral ischemia-reperfusion injury. *Redox Biol*. 2021;38:101792. doi:10.1016/j.redox.2020.101792
70. Wang Z, Zhou W, Dong H, Ma X, He Z. Dexmedetomidine pretreatment inhibits cerebral ischemia/reperfusion-induced neuroinflammation via activation of AMPK. *Mol Med Report*. 2018;18(4):3957–3964. doi:10.3892/mmr.2018.9349